Flex Printed Circuit Board Implemented Graphene-Based DNA Sensor for Detection of SARS-CoV-2

Samar Damiati, *Member, IEEE*, Sindre Søpstad, Martin Peacock, Ahmad S. Akhtar, Inês Pinto, Ruben R. G. Soares, and Aman Russom

***Abstract*—Since the COVID-19 outbreak was declared a pandemic by the World Health Organization (WHO) in March 2020, ongoing efforts have been made to develop sensitive diagnostic platforms. Detection of viral RNA provides the highest sensitivity and specificity for detection of early and asymptomatic infections. Thus, this work aimed at developing a label-free genosensor composed of graphene as a working electrode that could be embedded into a flex printed circuit board (FPCB) for the rapid, sensitive, amplification-free and label-free detection of SARS-CoV-2. To facilitate liquid handling and ease of use, the developed biosensor was embedded with a user-friendly reservoir chamber. As a proof-of-concept, detection of a synthetic DNA strand matching the sequence of ORF1ab was performed as a two-step strategy involving the immobilization of a biotinylated complementary sequence on a streptavidin-modified surface, followed by hybridization with the target sequence recorded by the differential pulse voltammetric (DPV) technique in the presence of a ferro/ferricyanide redox couple. The effective design of the sensing platform improved its selectivity and sensitivity and allowed DNA quantification ranging from 100 fg/mL to 1 μg/mL. Combining the electrochemical technique with FPCB enabled rapid detection of the target sequence using a small volume of the sample (5-20 μL). We achieved a limit-of-detection of 100 fg/mL, whereas the predicted value was ~33 fg/mL, equivalent to approximately 5 x 10^5 copies/mL and comparable to sensitivities provided by isothermal nucleic acid amplification tests. We believe that the developed approach proves the ability of an FPCB-implemented DNA sensor to act as a potentially simpler and more affordable diagnostic assay for viral infections in Point-Of-Care (POC) applications.**

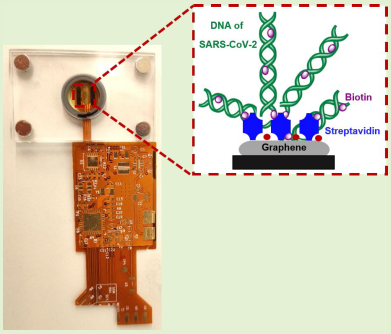

***Index Terms*— DNA, graphene, flex printed circuit board (FPCB), SARS-CoV-2, streptavidin–biotin complex.**

I. Introduction

THE rapid spread of the severe acute respiratory syndrome coronavirus-2 (SARS-CoV-2) and fatal progression of the coronavirus infectious disease (COVID-19) has attracted increasing concern globally, particularly because of expectations that the virus will continue to spread and might become a common seasonal infection. To date, no vaccines or effective drugs have been made available against COVID-19, and hence, early diagnosis is critical to control the outbreak. As a new virus with the ability to mutate, building an efficient diagnostic platform that allows rapid, sensitive, and selective detection is a challenging task, especially due to the limited knowledge available about SARS-CoV-2.

Development of Point-Of-Care (POC) devices with low limit-of-detection (LoD) enables early detection and confirms non-communicable levels of disease post-infection. Currently, PCR is the standard assay used globally to detect SARS-CoV-2 in respiratory samples. It is well known that nucleic acid amplification tests represent one of the most effective biosensing approaches for viral diagnostics due to their ability to chemically amplify the target and their high sensitivity. However, the technical complexity involved in rapid temperature cycles and low stability of enzymes hinders their effective translation into POC platforms. On the other hand, electrochemical methods are exploited in POC devices

Manuscript received January 30, 2021; revised March 1, 2021; accepted March 23, 2021. Date of publication March 24, 2021; date of current version June 14, 2021. The associate editor coordinating the review of this article and approving it for publication was Dr. Pantelis Georgiou. *(Corresponding authors: Samar Damiati; Aman Russom.)*

Samar Damiati is with the Department of Biochemistry, Faculty of Science, King Abdulaziz University, Jeddah 21589, Saudi Arabia, and also with the Division of Nanobiotechnology, Department of Protein Science, Science for Life Laboratory, KTH Royal Institute of Technology, 171 21 Stockholm, Sweden.

Sindre Søpstad is with the Department of Microsystems, Faculty of Technology, Natural Sciences and Maritime, University of South-Eastern Norway, 3184 Borre, Norway.

Martin Peacock is with Zimmer and Peacock Ltd., Royston SG8 9JL, U.K.

Ahmad S. Akhtar, Inês Pinto, Ruben R. G. Soares, and Aman Russom are with the Science for Life Laboratory, Division of Nanobiotechnology, Department of Protein Science, School of Engineering Sciences in Chemistry, Biotechnology and Health, KTH Royal Institute of Technology, 114 28 Stockholm, Sweden.

Digital Object Identifier 10.1109/JSEN.2021.3068922

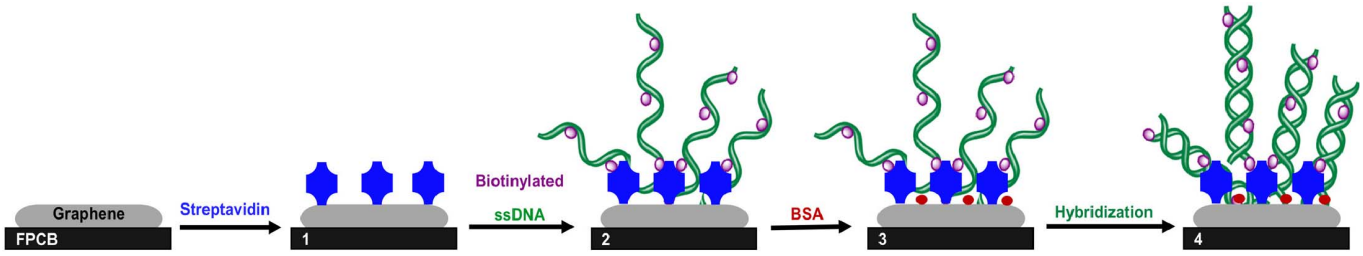

Fig. 1. Step-by-step illustration of the assay design and experimental setup in detection of a synthetic DNA sequence of SARS-CoV-2. (1) FPCB-implemented graphene electrode modified with streptavidin, (2) functionalization with biotinylated ssDNA capture sequence, (3) blocking with BSA, and (4) capture of target DNA.

that offer several advantages compared with other diagnostic techniques, namely, simplicity, speed of use, low cost, and high selectivity and sensitivity [1]–[3]. Promising strategies based on integration of electrodes into printed circuit boards (PCBs) are emerging as a potential mass-manufacturing technology for mechanically robust, long-standing, cost effective, and versatile platforms for (bio)chemical sensing [4], [5]. The performance of such setups depends on immobilized biomolecules which functionalize the working electrode integrated into the PCB. In addition to successful assembly of biomaterials onto the sensing matrix, fabricating an efficient electrochemical biosensor also depends on the electrode material [6]. Hence, exploiting biocompatible materials, such as polymers, graphene, and carbon nanotubes, in the biosensor industry is growing due to their stability, flexibility, low cost, and compatibility with various detection techniques [7], [8].

Ongoing efforts to develop diagnostic devices for COVID-19 based on various detection techniques are achieving significant progress globally. Although several COVID-19 tests have been approved by the Emergency Use Authorization (EUA) authority, determination of an optimal reference standard to identify clinical sensitivities is still not available. Furthermore, approved nucleic acid amplification and antigen diagnostic assays for SARS-CoV-2 vary up to 10,000-fold and exhibit significant variations in clinical sensitivity among various detection tests [9]. An interesting COVID-19 Ag Respi-Strip was developed by Coris BioConcept. This immune-chromatographic test (ICT) enabled rapid detection of the SARS-CoV-2 antigen in ∼15 min with LoD 250 pg/mL [10]. The surface plasmon resonance (SPR) technique was also used to detect SARS coronaviral surface antigen (SCVme). The designed SPR chip functionalized with the anti-SCVme antibody exhibited an LoD of 0.2 μg/mL [11]. In addition, a fabricated microfluidic ELISA platform was used by Tan *et al.* to detect SARS-CoV-2 S1 antigen and SARS-CoV-2 S1 antibody with LoD of 0.4 and 0.2 ng/mL, respectively, in a microliter sample volume [12]. Because it is a new epidemic, reported studies on the detection of SARS-CoV-2 using electrochemical approaches are limited. In a study reported by Seo *et al.*, a graphene-based field-effect transistor (FET)-based biosensing device functionalized with antibody against SARS-CoV-2 spike protein was developed. Authors achieved LoD = 1 and 100 fg/mL in PBS and clinical transport medium, respectively [13].

Graphene is a 2D sheet of carbon atoms that are arranged hexagonally and exposed on its surface [14]. Graphene has been employed in many biosensing platforms due to its high electronic conductivity, large specific area, and high carrier mobility. Further, biocompatibility, chemical stability, and low electrical noise make graphene a promising platform for a variety of sensing applications [15], [16]. Graphene electrodes can be functionalized with a synthetic ssDNA sequence to act as a probe that allows hybridization with ssDNA target. In this study, flex printed circuit board (FPCB)-implemented graphene and a biotinylated ssDNA capture sequence immobilized on a streptavidin surface were exploited in the design of a platform to detect a synthetic DNA strand matching the sequence of ORF1ab of SARS-CoV-2 in a label-free approach (Fig. 1). Streptavidin is a neutral protein that can bind up to four biotin molecules to generate the streptavidin–biotin complex which is one of the strongest non-covalent interactions in nature [17]. In the proposed detection platform, the capture ssDNA sequence of SARS-CoV-2 was conjugated with biotin to obtain a biotinylated probe that was subsequently immobilized onto the streptavidin-modified graphene surface. The generated sensing matrix was used for the hybridization of target DNA. Further, a user-friendly reservoir chamber module was designed to facilitate the delivery of sample solution to the working electrode of the FPCB device.

II. Components and Methods

A. Materials

Synthetic capture and target ssDNA sequences for SARS-CoV-2 were purchased from Integrated DNA Technologies (IDT). Unconjugated recombinant streptavidin (1 mg) was purchased from Thermo Fisher Scientific (Product Code 21122). Capture ssDNA sequences were modified with amine groups using Label IT Nucleic Acid Labeling Kit from Mirus Bio (Madison, WI, USA), followed by biotin labeling using EZ-Link NHS-Biotin Kit from Thermo Fisher Scientific. Saline-sodium citrate (SSC) buffer was purchased from Invitrogen as a 20x concentrate (3.0 M NaCl, 0.3 M sodium citrate, pH 7.0). Phosphate-buffered saline (PBS) tablets (1 tablet/200 mL deionized water, pH 7.2-7.6, Cat. No. P4417), Bovine serum albumin (BSA, Product Code A7906-50G), $K_3[Fe(CN)_6]$ (Cat. No. 60299), $K_4[Fe(CN)_6]$ (Cat. No. P3289), KCl, and Dimethylsulfoxide (DMSO) were obtained from Sigma-Aldrich GmbH, Germany. 1xTE solution (10 mM Tris, 0.1 mM EDTA, pH 8.0) was purchased from IDT.

B. FPCB and Reservoir Chamber Module Design and Fabrication

A flexible printed circuit (FPC) with integrated graphene electrodes was developed by Zimmer & Peacock Ltd., UK. Working (graphene), reference (silver/silver-chloride) and counter (carbon) electrodes were screen-printed directly onto the FPC. The module is a stamp-sized electronics platform designed for detection of electrochemical sensor signals (Fig. 2). The FPC carries analog front-ends for sensor conditioning and readout, a set of integrated screen-printed electrodes, and the ability to interface external electrodes. The integrated electrodes were printed using a graphene ink (PCT GC 01, Perpetuus Advanced Materials PLC, UK).

In order to prevent evaporation of the sample during the incubation and measurement processes, a microfluidic module with sealed chamber for the electrode was fabricated (Fig. 2a & 2b). The module was designed using Autodesk Fusion 360 (Education License) and then cut using computer-numerical-control milling machine (Roland Modela MDX-40A). The module consisted of two PMMA sheets cut into rectangles (36 mm × 22 mm × 2 mm) to serve as the top and bottom layer. A slot for O-ring (Nitrile Rubber O-Ring; I.D = 7.93 mm; O.D = 11.12 mm; RS PRO Article #689-625) was carved in the top and bottom layers. A chamber having a depth of 1.5 mm and 7 mm diameter was carved in the top layer. Two holes (1 mm dia.) at the top of the chamber served as inlet and vent for loading sample into the chamber. In order to align and close the two layers tightly, four slots for magnets (Neodymium magnet; Width 4 mm; Thickness 1 mm; RS PRO Article # 909-3641) on each corner of the top and bottom layer were carved and magnets were glued into the slots. As the magnets align and attach, a sealed chamber is formed around the electrode (Fig. 2c). The fabricated chamber is a user-friendly that allows sample injection up to 20 μL by simple manual pipetting without further need for an external pump.

C. Biotinylation of Capture ssDNA Sequence

A synthetic ssDNA sequence corresponding to 140 bp of the ORF 1ab region of SARS-CoV-2 virus (GCG AGC AAG AAC AAG TGA GGC CAT AAT TCT AAG CAT GTT AGG CAT GGC TCT ATC ACA TTT AGG ATA ATC CCA ACC CAT AAG GTG AGG GTT TTC TAC ATC ACT ATA AAC AGT TTT TAA CAT GTT GTG CCA ACC ACC ATA GA) was modified in a 2-step process comprising first the introduction of amine groups to enable a subsequent biotinylation using *N*-Hydroxysuccinimide (NHS) activated biotins. The amination reaction was performed according to the instructions of the labeling kit (Label IT Nucleic Acid Labeling Kit, Mirus Bio). Briefly, a ratio of 0.5:1 (v:w) of Label IT® Modifying Reagent to nucleic acid was used to label 5 μg of ssDNA with an initial concentration of 1 mg/mL. The reaction was incubated at 37°C for 1h, resulting in a labeling density of ∼1 amine group per 20-60 bases of ssDNA. The amine-conjugated ssDNA was then purified using centrifugal purification columns provided in the kit and buffer-exchanged into PBS using Amicon filter devices (10 KDa cutoff). For

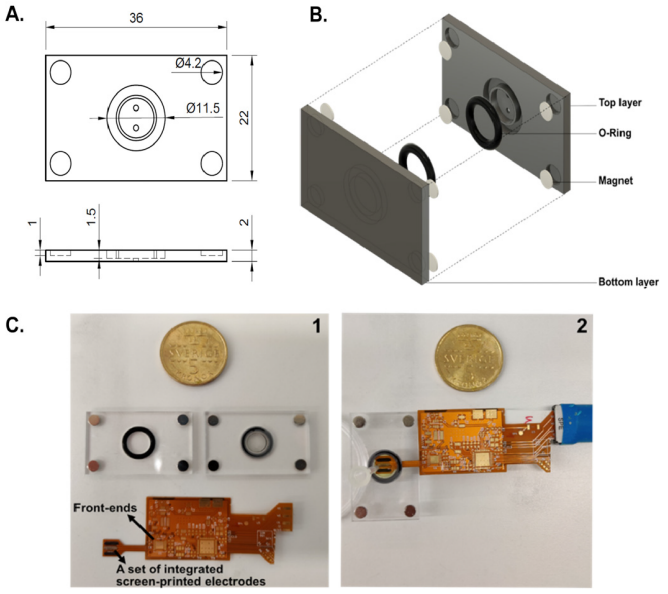

Fig. 2. **a.** CAD drawing (all dimensions are in mm) and **b.** schematic representation of the reservoir chamber module. **c.** **(1)** the bare FPCB device and disassembled chamber, and **(2)** the fully integrated FCPB platform into the chamber module.

the biotinylation reaction, a 10 mM solution of NHS-activated biotin was freshly prepared in DMSO and added at a ratio of 1:10 (v/v) to the purified amine-modified ssDNA solution (250 μg/mL). The reaction was incubated in the dark for 2h with continuous agitation. Finally, the unreacted biotin was washed away using Amicon filter devices (10 KDa) with TE buffer and the final concentration of pure biotinylated ssDNA was adjusted to 10 μg/mL.

D. Biosensing Assay

The graphene electrode of FPCB was immobilized with 300 μg/mL streptavidin in PBS. After overnight incubation at 4°C in a wet chamber, the working zone was rinsed three times with PBS to remove excess streptavidin. Subsequently, the electrode was incubated with biotinylated ssDNA capture probe for 60 min to form streptavidin-biotin complex and followed by rinsing step, twice with TE buffer and once with PBS, to remove unbound molecules. Free surface sites were then blocked using 1% BSA in PBS (pH 7.4) for 45 min to minimize unspecific adsorption on the functionalized surface. A washing step with PBS was conducted three times to remove excess BSA. The developed sensor was evaluated by measuring the cyclic voltammetry (CV) for each added layer. Cyclic voltammograms were recorded from −0.3 to 0.6 V at scan rate of 50 mV/s.

The functionalized electrode was then used to detect the target 195 bp synthetic ssDNA matching the ORF 1ab sequence of SARS-CoV-2. Different concentrations of the complementary target sequence (GTA GTA ATT GGA ACA AGC AAA TTC TAT GGT GGT TGG CAC AAC ATG TTA AAA ACT GTT TAT AGT GAT GTA GAA AAC CCT CAC CTT ATG GGT TGG GAT TAT CCT AAA TGT GAT AGA GCC ATG CCT AAC ATG CTT AGA ATT ATG GCC TCA CTT GTT

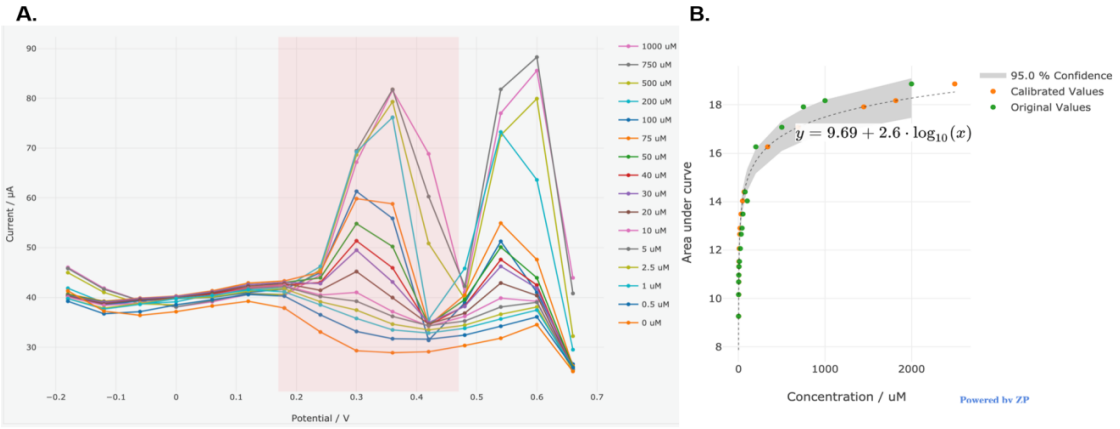

Fig. 3. (a) Coarsely-stepped differential pulse voltammograms and (b) fitting model for $[Fe(CN)_6]^{3-/4-}$ concentrations ranging from 1 mM to 2000 mM.

CTT GCT CGC AAA CAT ACA ACG TGT TGT AGC TTG TCA CAC CGT) in 2× SSC buffer (pH 7) were used to prepare the calibration curve and a non-complementary ssDNA sequence, corresponding to 140 bp of the E gene of the SARS-CoV-2 virus, was used as a control (CAA TAT TGC AGC AGT ACG CAC ACA ATC GAA GCG CAG TAA GGA TGG CTA GTG TAA CTA GCA AGA ATA CCA CGA AAG CAA GAA AAA GAA GTA CGC TAT TAA CTA TTA ACG TAC CTG TCT CTT CCG AAA CGA ATG AGT ACA TC). Hybridization reaction was performed at 37°C for 30 min. A washing step with 1× SSC was carried out three times after hybridization process. Differential pulse voltammetric (DPV) measurements were recorded from −0.2 to 0.8 V with a pulse amplitude of 50 mV and width of 50 ms. All electrochemical measurements (CV and DPV) were performed in 0.01 M PBS (pH 7.4) buffer containing 5 mM of ferro/ferricyanide ($[Fe(CN)_6]^{3-/4-}$) redox couple and 0.1 M KCl. The DPV current changes corresponding to target ssDNA sequence hybridizing to capture ssDNA sequence were calculated using the equation (1):

$$\Delta I = \frac{I_{SS}DNA}{I_{ds}DNA} \tag{1}$$

where $I_{SS}DNA$ and $I_{ds}DNA$ are the currents measured before and after hybridization with different target concentrations, respectively. To predict limit of detection (LoD) and relative standard deviation (RSD) the following formulas were used:

$$LoD = 3.3 \times \frac{\text{Standard deviation of the response of the curve}}{\text{Slope of the calibration curve}} \tag{2}$$

$$\%RSD = \frac{\text{Standard deviation}}{\text{Average}} \times 100 \tag{3}$$

III. Results and Discussion

Proof-of-principle

Proof-of-principle on the FPC was performed by running coarsely-stepped DPV (CSDPV) at diminishing concentrations of $[Fe(CN)_6]^{3-/4-}$, emulating the signal reduction caused by the blocking assay (Fig. 3). Despite the choppy shape of the voltammograms, the clear distinction between different concentrations demonstrates that the assay is compatible with a low-cost prototype. Furthermore, it adds to the evidence burden that the precise instrumental regime under which the assay is characterized is not necessarily required for the end application.

The (coarsely-stepped) square wave voltammetric (CSSVW) has previously been employed in determination of capsaicinoid content of chili derived food products [18], solid-state pH determination through open-circuit potentiometry, and chloride level quantification using square wave amperometric (SWA) detection [19]. The flex circuit leverages mature, and thus inexpensive, fabrication techniques like screen-printing, printed circuit board technology and off-the shelf components offer promising detection platforms for various infectious threats.

A. Electrochemical Behavior of the Fabricated FPCB-Implemented DNA Sensor

To verify the assembly processes of the modified sensor, cyclic voltammogramms were recorded sequentially in PBS containing 5mM $[Fe(CN)_6]^{3-/4-}$ redox couple (Fig. 4). The bare graphene surface showed the highest peak current which gradually declined after layer-by-layer modifications. The peak current of the bare graphene electrode decreased from 74.44 μA to 64.09 μA after being coated with streptavidin, which corresponded to ∼14%. Furthermore, incubating the modified electrode with the biotinylated capture ssDNA sequence of SARS-CoV-2 and blocking with BSA led to further reduction in the current. A final modification step was conducted and the peak current was reduced to 26% compared to the bare surface. Coating the graphene electrode with streptavidin and further biotin–streptavidin interaction in addition to blocking the surface with BSA hindered the electron transfer of $[Fe(CN)_6]^{3-/4-}$ onto the sensor surface and attenuated redox peaks because formed layers acted as physical barriers to the redox couple. These results demonstrate the role of streptavidin and biotin as non-conductive bioactive molecules that influence the electron transfer rate. Compared to uncharged graphene, streptavidin, biotin, and

TABLE I
COMPARISON OF REPORTED BIOSENSORS FOR SARS-CoV-2 DETECTION

Biosensing Platform	Detection method	LoD	Ref.
Abbott RealTime SARS-CoV-2 EUA	PCR	~100 copies of viral RNA per milliliter in nasopharyngeal swab	9
COVID-19 Ag Respi-Strip (nitrocellulose_ Au NPs_monoclonal Abs)	ICT	250 pg/mL in nasopharyngeal specimens	10
Au_GBP-E-SCVme fusion protein_Anti-SCVme Abs	SPR	0.2 µg/mL in PBS	11
anti-His tag Ab_SARS-CoV-2 or SARS-CoV S1 protein_anti- S1 IgG_HRP-conjugated secondary Ab	ELISA	0.4 and 0.2 ng/mL for SARS-CoV-2 S1 protein and SARS-CoV S1, respectively, in 10 times diluted human serum	12
Graphene_PBASE linker_SARS-CoV-2 Abs	FET	1 fg/mL in PBS 100 fg/mL in clinical transport medium 2.42×10^2 copies/mL in clinical samples	13
Graphene_Streptavidin_Biotinylated ssDNA	DPV	100 fg/mL in PBS	This study

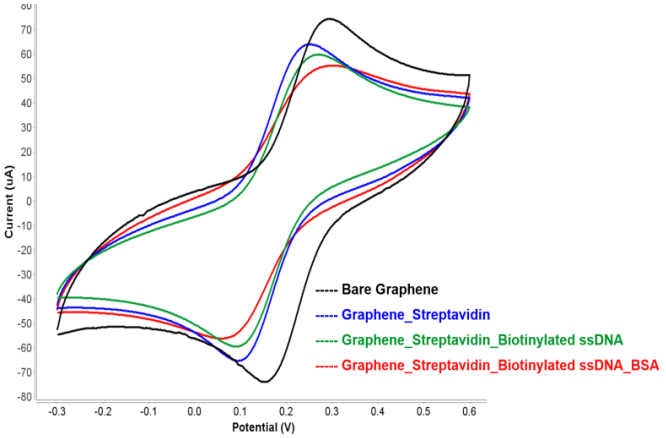

Fig. 4. Cyclic voltammograms at different steps of FPCB-implemented DNA sensor modifications on graphene working electrode. Electrochemical CV responses were recorded in PBS containing 5 mM $[Fe(CN)_6]^{3-/4-}$ solution at a scan rate of 50 mV/s.

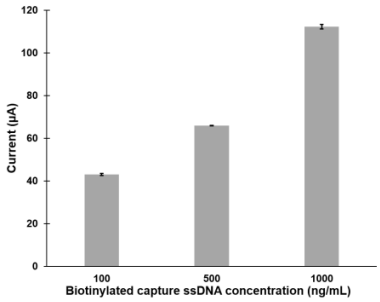

Fig. 5. Optimization of the concentration of the capture ssDNA sequence for SARS-CoV-2. Current changes recorded by DPV analysis after hybridization of the complementary DNA sequence of SARS-CoV-2 with an immobilized biotinylated ssDNA capture probe on a streptavidin-modified graphene sensor. Experimental conditions were as follows: target DNA concentration: 10 pg/mL in 2 × SSC; hybridization time: 30 min; voltammetric technique: DPV recorded from −0.2 to 0.8 V with a pulse amplitude of 50 mV and pulse of 50 ms.

DNA carry negative charges [20]. This may explain the slight peak shift towards negative voltage observed after modifying the electrode surface, which repelled the negatively charged redox probe ($[Fe(CN)_6]^{3-/4-}$) and decreased the electron transfer rate of redox couple. However, the current densities of each modified layer confirmed the successful modification of the sensor with biolayers comprising streptavidin and biotinylated ssDNA capture sequence.

The density of the capture DNA probe plays a critical role in the biosensor sensitivity. An even distribution of the capture probe and optimum spacing between probes onto the recognition layer are crucial to minimize steric hindrance upon hybridization with the target DNA sequence and enhance sensor performance [4], [21]. Although low or insufficient concentration of captured molecules significantly influences the detection sensitivity of the fabricated sensor, a high concentration of captured molecules can also affect the capture of the target molecule. A condensed and saturated surface can act as a steric barrier that blocks the $[Fe(CN)_6]^{3-/4-}$ redox system from transferring on the electrode surface, subsequently causing an indiscernible signal change [22]. Therefore, to optimize the capture ssDNA probe concentration, three different concentrations were evaluated (100, 500, 1000 ng/mL) with 10 pg/mL of target DNA (Fig. 5). Increasing the capture probe concentration led to an increase in the peak current monitored by DPV, which peaked at 1000 ng/mL, and hence was selected for further sensor evaluation steps.

The capture probe used in this study was modified with multiple biotin groups, which were randomly distributed along the backbone. Thus, immobilization on the streptavidin-coated surface is expected to result in a vertically/horizontally-oriented binding of the capture probes, allowing an efficient exposure of the complete sequence to the complementary sequence (target). Considering the possibility of the target DNA undergo some degradation prior to detection, the use of a relatively long capture probe is also advantageous over shorter oligo sequences (e.g. 35 or 70 bases), as the generated fragments would hybridize more efficiently to a longer sequence covering all possible random fragmentation events. On the other hand, shorter sequences are more likely to be only partially complementary to the fragments.

B. Analytical Performance of the Developed Sensor

The response of DPV was recorded upon capture of different concentrations of the complementary DNA sequence,

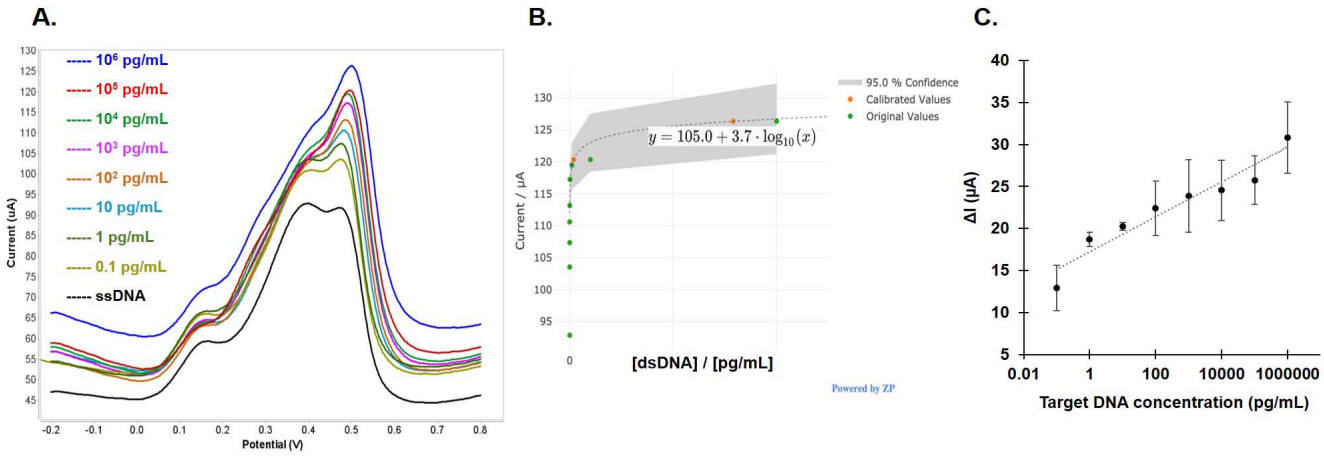

Fig. 6. **(a)** DPV responses and **(b)** fitting curve after probe hybridization assays using biotinylated ssDNA probe to target the complementary DNA sequence of SARS-CoV-2 at various concentrations (0.1, 1, 10, 10^2, 10^3, 10^4, 10^5, 10^6 pg/mL). **(c)** Plot of dependency of ΔI versus logarithm of several concentrations of target DNA.

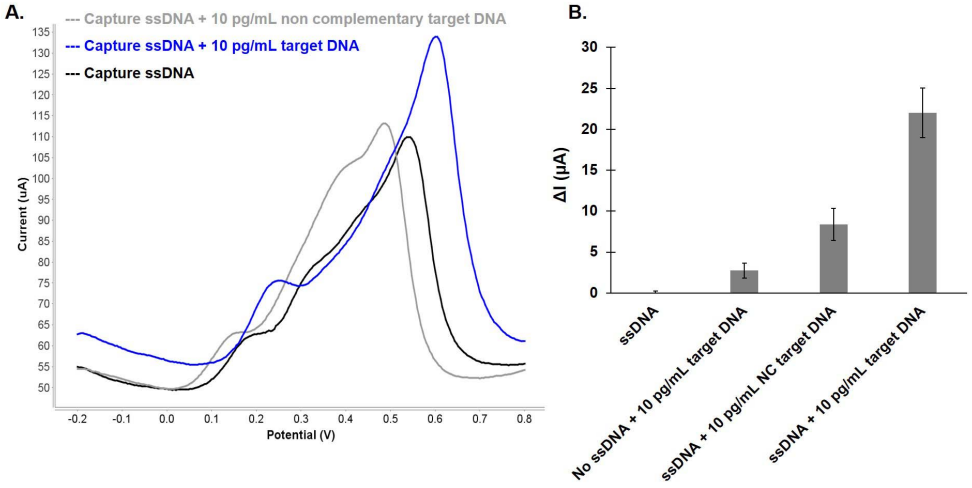

Fig. 7. **(a)** DPV curves obtained against the blank (capture ssDNA without target DNA), 10 pg/mL of non-complementary target DNA, and 10 pg/mL of complementary target DNA sequence SARS-CoV-2. **(b)** Changes of the DPV responses against capture ssDNA sequence only, 10 pg/mL of complementary DNA incubated in the absence of capture ssDNA, 10 pg/mL of non-complementary DNA, and 10 pg/mL of complementary target DNA SARS-CoV-2.

ranging from 0.1 to 10^6 pg/mL. Figure 6a shows that the DPV response gradually increased with increasing target DNA concentration. The current change (ΔI) was in proportion to the logarithm of the concentration of the target DNA sequence. The best regression coefficient obtained after fitting was $R^2 = 0.883$ and a good linearity was obtained for the calibration plot of hybridization of the capture ssDNA to the target ssDNA (Fig. 6b & 6c). The regression equation of the calibration curve was $\Delta I\ (\mu A) = 17.19 + 0.905\ \lg\ Conc_{target}$ (pg/mL) with a correlation coefficient (r^2) of 0.92. The calculated LoD was 32.88 fg/mL, equivalent to 5×10^5 cop/uL and comparable to sensitivities provided by nucleic acid tests using loop-mediated isothermal amplification (LAMP), where LoDs are typically in a range of $10^4 - 10^5$ copies per mL [23]. The good reproducibility of the developed biosensor was confirmed by the calculated %RSD value (1.002%) using three different detections at a target concentration of 10pg/mL. The high sensitivity of the DPV technique, in addition to the high conductivity of graphene, improve sensor sensitivity due to a high surface area and efficient electron transfer system. Table I shows the LoD for recently reported biosensors to detect SARS-CoV-2 using various detection methods.

The magnitude of the sensor response for a blocking assay typically has a negative correlation to the analyte concentration. This is a function of increased surface coverage, and thus fewer available reactive surface sites, or a net longer mean free diffusion path. This is not the case for the present assay, where a strong positive correlation between peak height before and after hybridization, ΔI, and analyte concentration, [DNA], is observed. One explanation to this could be that the hybridization changes the net charge of the DNA layer, and thus the electrostatic interaction between neighboring strands, and charged species in solution. For example, for an increased local salinity, surface bound DNA strands reduces their angle from being roughly perpendicular to around ∼40° for the saturated case [24]. The reduction in angle creates a shorter

diffusion path, which, for a diffusion limited electrochemical system, will amplify the response for a large number of hybridizations compared to that of a smaller.

C. Selectivity Studies

To validate the selectivity of the developed sensor, the biotinylated ssDNA capture sequence was incubated with 10 pg/mL of either non-complementary or complementary target DNA. Furthermore, the complementary DNA sequence was introduced to a fabricated sensor lacking the capture ssDNA sequence (Fig. 7a). A small current change was observed upon addition of the non-complementary DNA sequence corresponding to ∼2.5%. The shift of the DPV curve may be attributed to non-specific adsorption onto the sensing surface. The percentage increased to 20% with the addition of a complementary DNA sequence, which confirmed the hybridization assay and selectivity (Fig. 7b). However, several factors influence sensor specificity, including lack of high recognition/capture biomolecules, crowded biological media, and the resolution to differentiate between specific and non-specific binding [4], [8]. Moreover, due to the high affinity of streptavidin–biotin binding, fabricated sensors based on biotinylated capture antibodies or ssDNA probes can be highly specific in complex biological samples [22].

IV. Conclusion

To our knowledge, we report for the first time the development of an FPCB-implemented DNA sensor for the hybridization-based detection of SARS-CoV-2. While synthetic ssDNA was used as a model of the viral RNA sequence, due to enhanced stability during device optimization, a comparable performance within the same LoD order of magnitude is expected for DNA-RNA hybridization. However, further efforts must be invested in characterizing the effect of matrix interference, i.e. saliva, sputum or collection medium on assay performance to evaluate RNA extraction requirements. Exploiting graphene as a working electrode due to its extraordinary properties, and the streptavidin–biotin interaction to immobilize a capture DNA probe due to their high affinity, improved the efficiency and specificity of the proposed diagnostic platform. In a proof-of-concept study, we successfully demonstrated the immobilization of SARS-CoV-2 sequence and subsequent hybridization with the target ssDNA sequence. This platform demonstrated the importance of careful design of the sensing architecture to achieve high selectivity and sensitivity under optimized conditions. Furthermore, the electrochemical approach combined with an FPCB allowed label-free, rapid, and sensitive detection of the target DNA sequence ranging from 0.1 to 10^6 pg/mL due to the high sensitivity of the DPV technique. Furthermore, the analytical performance of the designed platform is not exclusive to the detection of SARS-CoV-2; the sensing matrix could be functionalized with various capture DNA sequences, resulting in the production of new diagnostic sensors for viruses and bacteria. The vision of flex circuit integrated with simple chamber is to provide a common platform for early product prototyping, such as to lower the often insurmountable barrier to in-field testing or commercialization.

Conflict of Interest

The authors declare that they have no conflict of interest.

Acknowledgment

The author Samar Damiati would like to thank embassy of Saudi Arabia in Stockholm, Sweden, and the cultural office of the royal embassy of Saudi Arabia in Berlin and Germany, for their kind support.

References

[1] D. Grieshaber, R. MacKenzie, J. Vörös, and E. Reimhult, "Electrochemical biosensors-sensor principles and architectures," *Sensors*, vol. 8, pp. 1400–1458, Mar. 2008.
[2] S. Damiati and B. Schuster, "Electrochemical biosensors based on S-layer proteins," *Sensors*, vol. 20, p. 1721, Jan. 2020.
[3] S. Damiati *et al.*, "Sensitivity comparison of macro- and micro-electrochemical biosensors for human chorionic gonadotropin (HCG) biomarker detection," *IEEE Access*, vol. 7, pp. 94048–94058, 2019.
[4] P. Jolly, J. Rainbow, A. Regoutz, P. Estrela, and D. Moschou, "A PNA-based Lab-on-PCB diagnostic platform for rapid and high sensitivity DNA quantification," *Biosensors Bioelectron.*, vol. 123, pp. 244–250, Jan. 2019.
[5] F. Güth, P. Arki, T. Löher, A. Ostmann, and Y. Joseph, "Electrochemical sensors based on printed circuit board technologies," *Procedia Eng.*, vol. 168, pp. 452–455, Jan. 2016.
[6] M. R. de Eguilaz, L. R. Cumba, and R. J. Forster, "Electrochemical detection of viruses and antibodies: A mini review," *Electrochem. Commun.* vol. 116, Jul. 2020, Art. no. 106762.
[7] J. A. C. Pérez *et al.*, "Bioinspired biomaterials and enzyme-based biosensors for point-of-care applications with reference to cancer and bio-imaging," *Biocatalys. Agricult. Biotechnol.*, vol. 17, pp. 168–176, Jan. 2019.
[8] S. Damiati, *Acoustic Biosensors for Cell Research* (Handbook of Cell Biosensors), G. Thouand, Ed. Cham, Switzerland: Springer, 2020.
[9] R. Arnaout *et al.*, "SARS-CoV2 testing: The limit of detection matters," *BioRxiv*, Jun. 2020, doi: 10.1101/2020.06.02.131144.
[10] P. Mertens *et al.*, "Development and potential usefulness of the COVID-19 ag respi-strip diagnostic assay in a pandemic context," *Frontiers Med.*, vol. 7, p. 225, May 2020.
[11] T. J. Park, M. S. Hyun, H. J. Lee, S. Y. Lee, and S. Ko, "A self-assembled fusion protein-based surface plasmon resonance biosensor for rapid diagnosis of severe acute respiratory syndrome," *Talanta*, vol. 79, no. 2, pp. 295–301, Jul. 2009.
[12] X. Tan, C. Lin, J. Zhang, and X. Fan, "Rapid and quantitative detection of COVID-19 markers in micro-liter sized samples," *BioRxiv*, Jan. 2020, doi: 10.1101/2020.04.20.052233.
[13] G. Seo *et al.*, "Rapid detection of COVID-19 causative virus (SARS-CoV-2) in human nasopharyngeal swab specimens using field-effect transistor-based biosensor," *ACS Nano.*, vol. 14, no. 4, pp. 5135–5142, 2020.
[14] D. R. Cooper *et al.*, "Experimental review of graphene," *Int. Scholarly Res. Notices*, vol. 2012, pp. 1–56, Jan. 2012.
[15] A. K. Geim and K. S. Novoselov, "The rise of graphene," *Nature Mater.*, vol. 6, no. 3, pp. 183–191, Mar. 2007.
[16] C. Haslam, S. Damiati, T. Whitley, P. Davey, E. Ifeachor, and S. Awan, "Label-free sensors based on graphene field-effect transistors for the detection of human chorionic gonadotropin cancer risk biomarker," *Diagnostics*, vol. 8, no. 1, p. 5, Jan. 2018.
[17] C. E. Chivers, A. L. Koner, E. D. Lowe, and M. Howarth, "How the biotin–streptavidin interaction was made even stronger: Investigation via crystallography and a chimaeric tetramer," *Biochem. J.*, vol. 435, no. 1, pp. 55–63, Apr. 2011.
[18] S. Søpstad, K. Imenes, and E. A. Johannessen, "Hybrid electrochemical sensor platform for capsaicin determination using coarsely stepped cyclic squarewave voltammetry," *Biosensors Bioelectron.*, vol. 130, pp. 374–381, Apr. 2019.
[19] S. Sopstad, K. Imenes, and E. A. Johannessen, "Chloride and pH determination on a wireless, flexible electrochemical sensor platform," *IEEE Sensors J.*, vol. 20, no. 2, pp. 599–609, Jan. 2020.
[20] S. Sivasankar, S. Subramaniam, and D. Leckband, "Direct molecular level measurements of the electrostatic properties of a protein surface," *Proc. Nat. Acad. Sci. USA*, vol. 95, no. 22, pp. 12961–12966, Oct. 1998.

[21] S. D. Keighley, P. Estrela, P. Li, and P. Migliorato, "Optimization of label-free DNA detection with electrochemical impedance spectroscopy using PNA probes," *Biosensors Bioelectron.*, vol. 24, no. 4, pp. 906–911, Dec. 2008.
[22] F. Islam *et al.*, "An electrochemical method for sensitive and rapid detection of FAM134B protein in colon cancer samples," *Sci. Rep.*, vol. 7, no. 1, Dec. 2017, Art. no. 133.
[23] A. Alekseenko *et al.*, "Direct detection of SARS-CoV-2 using non-commercial RT-LAMP reagents on heat-inactivated samples," *Sci. Rep.*, vol. 11, no. 1, Dec. 2021, Art. no. 1820.
[24] J. Ambia-Garrido, A. Vainrub, and B. M. Pettitt, "A model for structure and thermodynamics of ssDNA and dsDNA near a surface: A coarse grained approach," *Comput. Phys. Commun.*, vol. 181, no. 12, pp. 2001–2007, Dec. 2010.

Samar Damiati (Member, IEEE) received the Ph.D. degree from the Department of Nanobiotechnology, Institute for Synthetic Bioarchitectures, University of Natural Resources and Life Sciences (BOKU), Vienna, Austria, in 2013. She is currently an Invited Researcher with the KTH Royal Institute of Technology, Stockholm, Sweden. She is on leave from the Biochemistry Department, King Abdulaziz University, Jeddah, Saudi Arabia. Her current research interests include development of synthetic bioarchitectures, fabrication of biosensors, and designing microfluidic devices for several applications.

Sindre Søpstad received the B.Eng. degree in electronics engineering, the M.Sc. degree in microsystems technology, and the Ph.D. degree in electrochemical microsystems from the University of Southeastern Norway (USN) in 2013, 2015, and 2019, respectively. Since 2012, he has been working with biosensor company Zimmer and Peacock, Horten, Norway. His research interests include span electrochemical sensor development, electronic front-end design, and automated data analysis.

Martin Peacock is an Industrial Bioelectrochemist with 20 years of biosensor experience, having industrial roles from Abbott Diabetes to GSK and solving technical challenges from continuous glucose monitoring to RNA analysis. He has set-up biosensor focused companies across the globe from Silicon Valley California to Oslo Norway.

Ahmad S. Akhtar received the bachelor's degree in electrical engineering from the National University of Science and Technology (NUST), Pakistan, in 2013, and the master's degree in microsystems engineering from the University of Freiburg, Germany, in 2017. He is currently pursuing the Ph.D. degree in biotechnology programme with the Royal Institute of Technology (KTH), Stockholm. He has experience in the field of microfluidics and biotechnology.

Inês Pinto received the Ph.D. degree in biotechnology and biosciences from Instituto Superior Técnico, Portugal, in 2018. She is currently a Postdoctoral Researcher with the Royal Institute of Technology in Stockholm, Sweden, working on microfluidic-based biosensing applications. Her research interests include immunoassay development for detection of protein biomarkers and nucleic acid rapid tests.

Ruben R. G. Soares received the Ph.D. degree in biotechnology and biosciences from the University of Lisbon in 2018. He is currently a Postdoctoral Researcher with the Science for Life Laboratory (SciLifeLab), Sweden, affiliated with Stockholm University and the Royal Institute of Technology (KTH). His current research focuses on the development and miniaturization of isothermal nucleic acid amplification assays based on rolling circle amplification for point of care pathogen diagnostics and improved screening of antimicrobial susceptibility at the genomic level, biosensor development, surface chemistry, microfluidics, and nano/micro-fabrication.

Aman Russom received the Ph.D. degree from KTH Royal Institute of Technology, Sweden, in 2005. From 2005 to 2008, he did his postdoctoral fellowship with Harvard Medical School. In 2008, he returned back to Sweden, where he is currently heading the Division of Nanobiotechnology, consisting of eight Ph.D. students and four post docs, with the Science for Life Laboratory, KTH Royal Institute of Technology. His current research is focused on applying engineering principles and technologies, especially micro-and nanotechnology, to clinical medicine with emphasis on point of care diagnostics.